Title
Vehicle Longitudinal Control Using Discrete Markers

Authors
Love, David W.
Tomizuka, Masayoshi

Publication Date
1994

CALIFORNIA PATH PROGRAM
INSTITUTE OF TRANSPORTATION STUDIES
UNIVERSITY OF CALIFORNIA, BERKELEY

Vehicle Longitudinal Control Using Discrete Markers

David W. Love
Masayoshi Tomizuka

California Partners for Advanced Transit and Highways (PATH)
Mechanical Engineering Department
University of California at Berkeley

California PATH Research Report
UCB-ITS-PRR-94-28

This work was performed as part of the California PATH Program of the University of California, in cooperation with the State of California Business, Transportation, and Housing Agency, Department of Transportation; and the United States Department of Transportation, Federal Highway Administration.

December 1994
ISSN 1055-1425

Vehicle Longitudinal Control Using Discrete Markers

David W. Love
Masayoshi Tomizuka

California Partners for Advanced Transit and Highways (PATH)
Mechanical Engineering Department
University of California at Berkeley
December 1994

Abstract

A hybrid observer is proposed as a method of estimating position and velocity of a vehicle when the primary input is a series of discrete magnetic markers placed along a roadway. For the preliminary studies, the vehicle was modeled as a pure inertial system with acceleration input. Two methods of determining the time t_k at which the k-th marker is passed are discussed, and simulations using both methods are shown. Compensation for errors arising due to inaccurate measurement of this time is proposed and validated. A Proportional-Integral-Derivative (PID) controller acting on error signals from the hybrid observer is also developed and simulated. An "optimal" trajectory for marker advance/fallback and velocity change commands is calculated and verified in simulation, and its effects on the PID controller are discussed.

Keywords: Advanced Vehicle Control Systems, Automatic Highway Systems, Control Systems, Intelligent Vehicle Highway Systems, Longitudinal Control, Point Follower Control, Roadway Guidance Markers.

Executive Summary

Vehicles in an Automated Highway System (AHS) have many levels of control, from high-level scheduling and platooning to hardware-specific controller design. One intermediate level of control involves the two basic maneuvering classes for vehicles in an Intelligent Vehicle Highway System (IVHS): lateral control and longitudinal control. Lateral control of a vehicle consists of lane following, lane changing, and similar maneuvers, and a fixed roadway reference system consisting of magnetic markers placed in the roadbed has been suggested as a method of aiding in these maneuvers. On the other hand, longitudinal control, comprised of velocity tracking, intra-platoon spacing control, and similar maneuvers, has until now relied on inter-vehicle spacing as determined by range sensors as the primary control input. This method has the obvious advantage of incorporating the distance between vehicles directly into controller design, but it also carries the disadvantage that any position errors in "downstream" vehicles will propagate through the platoon, leading to a consequence known as the "slinky" effect.

This report investigates the feasibility of using the magnetic markers, already present for lateral vehicle guidance, for longitudinal control. Instead of using a "vehicle-follower" method implied by relying on direct inter-vehicle distance measurement, the use of the magnetic markers gives a "point-follower" scheme, relying on a fixed reference system. This method would not be susceptible to the "slinky" effect or other vagaries of a vehicle-follower system, and could be implemented relatively inexpensively if the magnetic marker structure is already in place. Since inter-vehicle spacing is still of extreme importance, a range sensor of some sort will still need to be installed on each vehicle; but if the discrete markers can be used for accurate vehicle location relative to the markers, the range sensors may be less accurate, hence less expensive, than if they were being relied on to provide exact spacing information.

This report assumes a simple vehicle model with acceleration input and measurements of the actual acceleration in addition to the magnetic marker measurements, and details the theoretical background behind the development of a "hybrid observer", a tool of primary

importance for the accurate estimate of position and velocity between markers. It also discusses the design of an optimal trajectory for vehicle velocity and position changes.

The results for this simple vehicle model are promising, though it becomes clear that accurate detection of the exact location of the markers is vital to the performance of any controller based on this point-follower method, especially at high velocities. If a constant-rate polling clock is used in the measurements, high velocities will lead to inaccurate state estimates, so the inclusion of a hardware peak detector might be necessary for accurate control. If the markers are accurately located, however, this study shows that they can indeed be used as a basis for longitudinal control of vehicles for IVHS.

Table of Contents

List of Figures

1.0 Concept and Motivation

Intelligent Vehicle Highway Systems (IVHS) have been the topic of several studies in recent years. The studies performed by the California Partners for Advanced Transit and Highways (PATH) have confirmed the viability of a discrete magnetic marker reference/sensing system for lateral control of a vehicle (Hessburg et al. 1991, Peng et al. 1992a,b). At present, longitudinal vehicular control within a platoon of closely spaced vehicles is being realized through a "vehicle follower" scheme (Chang and Georghiades 1992, Chien and Ioannou 1992, Hedrick et al. 1991, McMahon et al. 1992). The spacing between vehicles is compared to a desired spacing, and this error is used as part of the control algorithm. This spacing is usually determined by an accurate distance measuring sensor. Figure 1.1 shows a schematic of the proposed system.

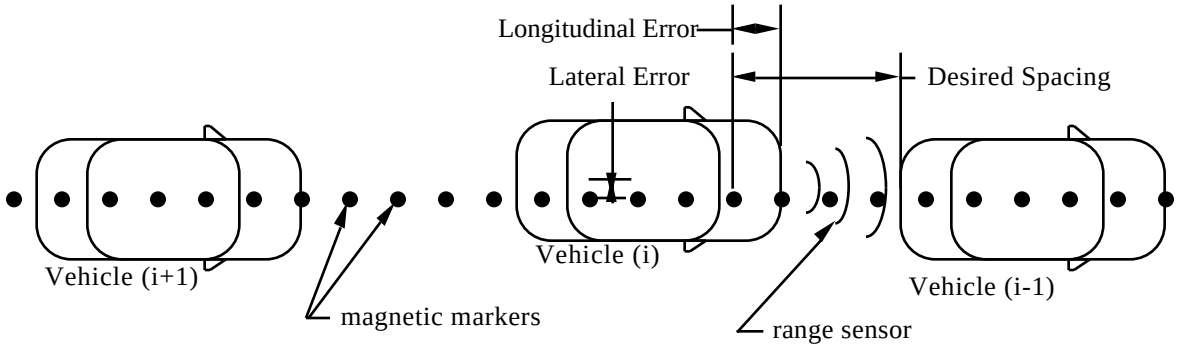

Figure 1.1 - System Visualization

One unfortunate effect of a vehicle follower method is the so-called "slinky" effect, which is a series of spacing oscillations that propagates throughout the platoon whenever any vehicle deviates from its proper position. Though methods have been proposed within the vehicle follower regime to eliminate this effect (Chien and Ioannou 1992), the magnetic marker reference/ sensing system motivates a "point follower" scheme as a viable alternative to or backup for longitudinal guidance. With this method, each vehicle measures position with respect to fixed markers rather than moving vehicles, and the "slinky" effect is not an issue. Even if this system is not used as the primary control input, it could be used as independent or backup measurements for the vehicle follower system.

The problem that is being investigated in this paper, then, is whether the discrete magnetic markers, which will already be present for lateral control, can be used for safe and reliable longitudinal control of a vehicle. If the only inputs (i.e., no tachometer measurements, accelerometer measurements, or other inputs) come from these discrete markers spaced at a distance ℓ along the roadway, this implies that

$$V_{average}(t_{k+1}) = \frac{\ell}{t_{k+1} - t_k} = \frac{\ell}{T_m} \qquad 1.1$$

is the best direct estimate of the true velocity. Because this measure is only the average velocity over the time interval between markers, inaccuracies will arise during acceleration and deceleration. Therefore, we assume that accurate acceleration measurements are available at all times. This assumption carries with it certain difficulties inherent in the use of any accelerometer, though these difficulties can be reduced by using tachometers placed on the wheels. For the first treatment of this problem, we used a pure inertial model that did not allow for wheel slip, so the use of a tachometer would have given trivial results and were not investigated. The model also included acceleration and jerk limits (rate limiter on acceleration), which will be shown to affect performance, but which make the behavior more realistic. This model does not take into account all of the complex dynamics of the vehicle, but it provides an acceptable framework upon which the controller design can be tested.

2.0 Hybrid Observer

Because this system has only discrete inputs, it makes sense to discretize the system with respect to the time between markers, $T_m = t_{k+1} - t_k$. However, this time will change depending on the vehicle velocity. Therefore, we propose a "hybrid" observer that uses a continuous predictor and a discrete corrector, to more accurately estimate the states between sampling instances. Assume a linear single-input-single-output system with states $\mathbf{x}(t)$, input $u(t)$, and output $y(t)$. If the state and output equations for the continuous system are assumed to be

$$\frac{d\mathbf{x}}{dt} = \mathbf{A}\,\mathbf{x}(t) + \mathbf{B}\,u(t) \quad \text{and} \quad y(t) = \mathbf{C}\,\mathbf{x}(t), \tag{2.1}$$

then the discretized state equations become

$$\mathbf{x}(t_{k+1}) = e^{\mathbf{A}(t_{k+1}-t_k)}\mathbf{x}(t_k) + \int_{t_k}^{t_{k+1}} e^{\mathbf{A}(t_{k+1}-\tau)}\mathbf{B}u(\tau)d\tau\,, \tag{2.2}$$

or, if the input u is constant over the interval between markers,

$$\mathbf{x}(t_{k+1}) = e^{\mathbf{A}(t_{k+1}-t_k)}\mathbf{x}(t_k) + \left(\int_{t_k}^{t_{k+1}} e^{\mathbf{A}(t_{k+1}-\tau)}\mathbf{B}d\tau\right)u(t_k)\,. \tag{2.3}$$

Given an estimate of $\mathbf{x}(t)$ at the k-th sampling time instance, $\hat{\mathbf{x}}(k|k)$, the evolution of $\mathbf{x}(t)$ until the next sampling time instance, k+1, is predicted by

$$\hat{\mathbf{x}}(t|t_k) = e^{\mathbf{A}(t-t_k)}\hat{\mathbf{x}}(k|k) + \int_{t_k}^{t} e^{\mathbf{A}(t-\tau)}\mathbf{B}u(\tau)d\tau\,. \tag{2.4}$$

At the (k+1)-th sampling instance, $t = t_{k+1}$, Eq. (2.4) gives

$$\hat{\mathbf{x}}(k+1|k) = \hat{\mathbf{x}}(t_{k+1}|t_k) = e^{\mathbf{A}(t_{k+1}-t_k)}\hat{\mathbf{x}}(k|k) + \int_{t_k}^{t_{k+1}} e^{\mathbf{A}(t_{k+1}-\tau)}\mathbf{B}u(\tau)d\tau \ . \qquad 2.5$$

This is an a priori estimate, made before information from the measurement at the (k+1)-th marker is utilized. Notice that the implementation of Eq. (2.4) and Eq. (2.5) requires the availability of u(t). For vehicle applications, this information is obtained from an accelerometer on board the vehicle. Furthermore, the wheel speed ω_w, which is normally available in any vehicle, can be utilized as an additional measurement to estimate the vehicle speed between markers. However, the direct velocity estimate from this rotation rate, $\mathbf{v}_w = R_w\omega_w$, is not an exact indication of the vehicle speed due to tire slip λ. Normally, the vehicle speed and wheel speed satisfy the relation

$$\frac{\mathbf{v}_w - \mathbf{v}}{\mathbf{v}_w} \approx \lambda. \qquad 2.6$$

Unless the vehicle accelerates or decelerates too rapidly, or there is a significant change in road condition (dry to icy asphalt, or gravel roads), the estimate

$$\hat{\mathbf{v}} \approx (1 - \lambda)\, \mathbf{v}_w \qquad 2.7$$

may be a good additional input to the observer. For this to be an effective input, a good estimate (or measurement) of the wheel slip must also be obtained. Investigation into this should be combined with a more detailed dynamic model which includes a wheel model, and is left as a future research item.

When the magnetic markers are equally spaced, the (k+1)-th measurement is

$$y(k+1) = (k+1)\ell + n(k+1), \qquad 2.8$$

where ℓ is the marker spacing, n(k) is the measurement noise, and it has been assumed that the counting of markers begins at $k = 0$. Then the equation for correcting the a priori estimate $\hat{\mathbf{x}}(k+1|k)$ is

$$\hat{\mathbf{x}}(k+1|k+1) = \hat{\mathbf{x}}(k+1|k) + \mathbf{L}\left[(k+1)\ell + \mathrm{n}(k+1) - \mathbf{C}\hat{\mathbf{x}}(k+1|k)\right], \qquad 2.9$$

where **L** is the observer gain matrix. A block diagram of the hybrid observer structure is shown in figure 2.1. The reset switch is for initializing the integrator output to $\hat{\mathbf{x}}(t|t_k)$ at every instance when the state estimate is updated by a newly measured y(t_k).

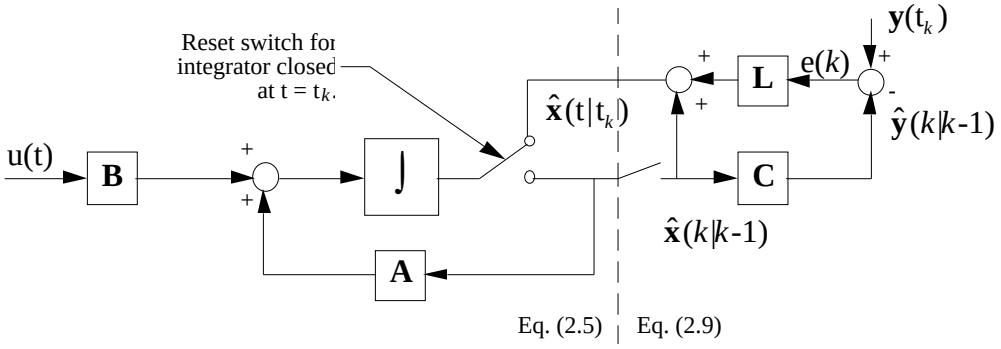

Figure 2.1 - Hybrid Observer Structure

The expression $(k+1)\ell$ can also be given by

$$(k+1)\ell = \mathbf{C}\mathbf{x}(t_{k+1}) = \mathbf{C}\left[e^{\mathbf{A}(t_{k+1}-t_k)}\mathbf{x}(t_k) + \int_{t_k}^{t_{k+1}} e^{\mathbf{A}(t_{k+1}-\tau)}\mathbf{B}\mathrm{u}(\tau)d\tau\right] \qquad 2.10$$

Combining Eq. (2.9) and Eq. (2.10), and defining the error $\mathbf{e}(k|k) = \mathbf{x}(k) - \hat{\mathbf{x}}(k|k)$, the error equation becomes

$$\mathbf{e}(k+1|k+1) = [\mathbf{I} - \mathbf{LC}]e^{\mathbf{A}(t_{k+1}-t_k)}\mathbf{e}(k|k) = [\mathbf{I} - \mathbf{LC}]\mathbf{A_d}\mathbf{e}(k|k), \qquad 2.11$$

where $\mathbf{A_d} = e^{\mathbf{A}(t_{k+1}-t_k)}$. If the values of **L** are chosen so that **[I - LC] $\mathbf{A_d}$** is asymptotically stable, it is guaranteed that the estimates will converge to the states.

For this simple (pure inertial) system, the two states are chosen to be x_1 = position, x_2 = velocity, and the position is used as the output. This gives, for acceleration input,

$$\mathbf{A} = \begin{bmatrix} 0 & 1 \\ 0 & 0 \end{bmatrix}, \quad \mathbf{B} = \begin{bmatrix} 0 \\ 1 \end{bmatrix}, \quad \mathbf{C} = \begin{bmatrix} 1 & 0 \end{bmatrix}. \tag{2.12}$$

For this model, $\mathbf{A_d}$ is given by

$$\mathbf{A_d} = \begin{bmatrix} 1 & T_m \\ 0 & 1 \end{bmatrix}, \tag{2.13}$$

where $T_m = t_{k+1} - t_k$. The matrix in the error equation (2.11) is

$$\mathbf{E} = [\mathbf{I} - \mathbf{LC}]\mathbf{A_d} = \begin{bmatrix} 1-\ell_1 & 0 \\ -\ell_2 & 1 \end{bmatrix}\begin{bmatrix} 1 & T_m \\ 0 & 1 \end{bmatrix} = \begin{bmatrix} 1-\ell_1 & (1-\ell_1)T_m \\ -\ell_2 & 1-T_m\ell_2 \end{bmatrix}, \tag{2.14}$$

where $\mathbf{L} = [\ \ell_1 \quad \ell_2\ ]^T$. The eigenvalues of this matrix can be found from

$$\det(\lambda \mathbf{I} - \mathbf{E}) = \lambda^2 - (2 - \ell_1 - T_m\ell_2)\lambda + (1 - \ell_1) = 0. \tag{2.15}$$

By assigning the eigenvalues of this error matrix, the response of the error equation can be determined. If the poles of **E** are assigned inside the unit circle in the z-plane, the response will be asymptotically stable with the characteristic equation

$$\lambda^2 - (p_1 + p_2)\lambda + p_1 p_2 = 0. \tag{2.16}$$

Equations (2.14) and (2.16) allow for solution of the observer gains ℓ_1 and ℓ_2 as

$$\begin{aligned} \ell_1 &= 1 - p_1 p_2 \\ \ell_2 &= \frac{(1-p_1)(1-p_2)}{T_m}. \end{aligned} \tag{2.17}$$

2.1 "Deadbeat" Response

In particular, if $p_1 = p_2 = 0$ (finite settling time or "deadbeat" response), the observer gains required for constant eigenvalue locations are

$$\ell_1 = 1 \text{ and } \ell_2 = \frac{1}{T_m}. \tag{2.18}$$

For this observer gain, the position estimate is

$$\hat{\mathbf{x}}_1 (k\,|k\,) = y(k) = k \times \ell. \tag{2.19}$$

Furthermore,

$$\hat{\mathbf{x}}_1(t|t_k) = \hat{\mathbf{x}}_1(k|k) + \int_{t_k}^{t} \hat{\mathbf{x}}_2(\tau\,|\,t_k)d\tau \quad \text{and} \quad \hat{\mathbf{x}}_2(t|\,t_k) = \hat{\mathbf{x}}_2(k|\,k) + \int_{t_k}^{t} \mathbf{u}(\tau)d\tau\ . \tag{2.20}$$

Setting $t = t_{k+1}$ in Eq. (2.20), we obtain

$$\hat{\mathbf{x}}_{\,1}(k+1|k) = \hat{\mathbf{x}}_{\,1}(t_{k+1}|t_k) \qquad \text{and} \quad \hat{\mathbf{x}}_{\,2}(k+1|k) = \hat{\mathbf{x}}_{\,2}(t_{k+1}|t_k). \tag{2.21}$$

At the (k+1)-th sampling instance, the estimate of the velocity then becomes

$$\hat{\mathbf{x}}_2(k+1|k+1) = \hat{\mathbf{x}}_2(k+1|k) + \frac{1}{T_m}[\ y(k+1) - \mathbf{C}\hat{\mathbf{x}}_1(k+1|k)]. \tag{2.22}$$

From Eq. (2.19) through (2.22), we find

$$\hat{\mathbf{x}}_2(k+1|k+1) = \hat{\mathbf{x}}_2(k|k) + \int_{t_k}^{t_{k+1}} \mathbf{u}(\tau)d\tau + \frac{1}{T_m}\left[(k+1)\ell - \left(\hat{\mathbf{x}}_1(k|k) + \hat{\mathbf{x}}_2(k|k)T_m + \int_{t_k}^{t_{k+1}}\int_{t_k}^{t} \mathbf{u}(\tau)d\tau\ dt\right)\right]$$

$$= \int_{t_k}^{t_{k+1}} \mathbf{u}(\tau)d\tau + \frac{1}{T_m}\left[\ell - \int_{t_k}^{t_{k+1}}\int_{t_k}^{t} \mathbf{u}(\tau)d\tau\ dt\right]. \tag{2.23}$$

This form of observer (with eigenvalues of $\mathbf{[I - LC]A_d}$ at 0) estimates the velocity based on the acceleration between subsequent markers, and is not tied directly to the position estimates. Although this makes it seem that the observer is not taking full advantage of accumulated history, this form does have certain advantages. One of these advantages is that the

observer for the velocity is essentially decoupled from the observer for the position. If the roots of the characteristic equation are not placed at the origin of the complex plane, it is not possible to decouple the velocity estimator from the position estimator. For control purposes, we are not truly interested in the actual position estimate as a measure of total longitudinal motion; this estimate simply continues to increase. Instead, we are interested in knowing how close the vehicle is relative to a moving "target", defined as a desired profile.

As far as this observer is concerned, we are not actually interested in where the other vehicles are; we are only concerned with how each vehicle is performing relative to its own desired position and velocity. That is the basis of the point-follower scheme: each vehicle follows a path relative to a fixed reference frame rather than a moving reference frame. Of course, for IVHS, we are greatly concerned with how far vehicles are from one another, so these position estimates (relative to markers) can be combined with rough range sensors to determine actual spacing between vehicles. There should also be inter-vehicle communication to relate problems when one vehicle fails to meet an expected level of tracking performance, possibly causing danger to other vehicles.

It is informative to check what Eq. (2.21) gives for special cases:

• No acceleration from k-th to (k+1)-th marker (u = 0). In this case,

$$\hat{x}_2(k+1|k+1) = \frac{\ell}{t_{k+1} - t_k} = \frac{\ell}{T_m}. \qquad 2.24$$

• Constant acceleration from k-th to (k+1)-th marker ($u = u_c$). In this case,

$$\hat{x}_2(k+1|k+1) = \frac{\ell}{T_m} + \tfrac{1}{2} u_c T_m. \qquad 2.25$$

2.2 Determination of t_k

For this report, the state update clock is assumed to be running at the same rate as the magnetometer polling clock, meaning that every time the magnetometer is checked to see if a

marker was passed, the state estimates were updated. This assumption is in accordance with past experiments with these magnetic markers (Peng et al. 1992b), which used an update period of 3 msec. However, the sampling time does not need to be equal to this value, nor does it have to be a fixed value; an increased sampling rate at higher velocities could improve measurement accuracy.

With this assumption of constant magnetometer polling, there are two different scenarios for defining t_k, the time at which a vehicle is informed that it has passed marker k. The first scenario assumes that the time when the vehicle passes a marker can be measured exactly. This can be done by adding a timer along with a peak detector for the magnetometer output. This time can be utilized immediately by interrupting other processor tasks, or it can be stored and used at the next "tick". The second scenario assumes only that a "marker passed" signal is generated whenever it is determined that a marker was passed sometime between the previous and current "tick". A schematic of these two scenarios is shown in figure 2.2 on the next page.

The first scenario gives exact information; if $x_2 = v_c$ is constant, then (in deadbeat response) $\hat{x}_2 := \frac{\ell}{T_m} = v_c$, and any error would be due only to sensor noise n. With the second scenario, however, there is a 3 msec "window" during which a marker is passed. This gives the value of T_m an inherent error of up to 3 msec, which is reflected in $\hat{x}_2$ (and the position estimate $\hat{x}_1$). And because T_m decreases with increasing velocity, the effect of this inherent error on the accuracy of the state estimates increases as the vehicle velocity increases. In this case, even constant-velocity travel will not be accurately estimated without some form of error correction.

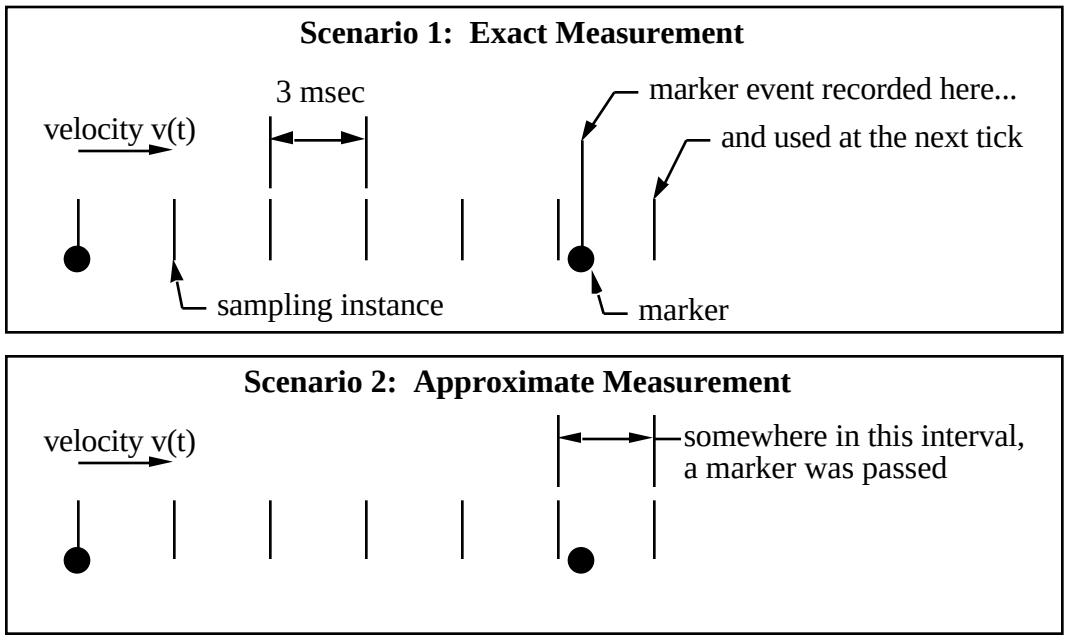

Figure 2.2 - Schematic of t_k Measurement Scenarios

In the sections that follow, we will compare simulations run under both measurement scenarios, and discuss in detail some difficulties encountered by employing the second scenario. We will also present methods which were implemented to improve the response and accuracy of the estimates under this scenario. It should be emphasized in advance that accurate measurement of t_k will be shown to be vital to the performance of the observer, and hence to any controller which uses its state estimates.

2.3 Preliminary Simulation Results

Simulations were performed on a variety of velocity profiles, but the two simplest profile types are shown in figure 2.3. Profile Type 1 represents an optimal trajectory for velocity change from v_1 to v_f, with maximum acceleration of 0.1 g. Profile Type 2 represents an optimal trajectory for marker advancement with maximum acceleration of 0.05 g and maximum jerk of 0.05 g/s. The magnetic marker spacing in all simulations was assumed to be 1 meter.

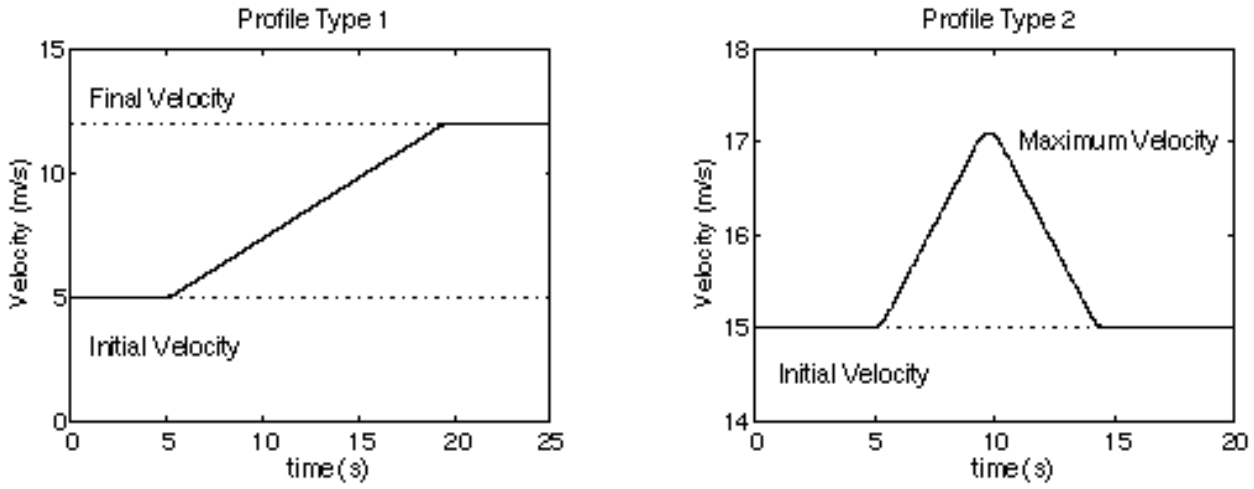

Figure 2.3 - Velocity Profiles

Results from simulations using one velocity change profile are shown in figures 2.4 and 2.5. For this velocity profile, v_f was chosen as 11.11 m/s. Since, in these simulations, the magnetometer is being sampled at intervals of dt = 3 msec, the marker spacing ℓ is an exact multiple of $v_f \times dt$. In other words, the magnetometer will take a measurement directly above each marker (or at the same position relative to each marker, for scenario 2), once a constant velocity is reached. Figure 2.4 shows the velocity error under scenario 1, in which t_k is determined "exactly", while figure 2.5 shows the velocity error under scenario 2.

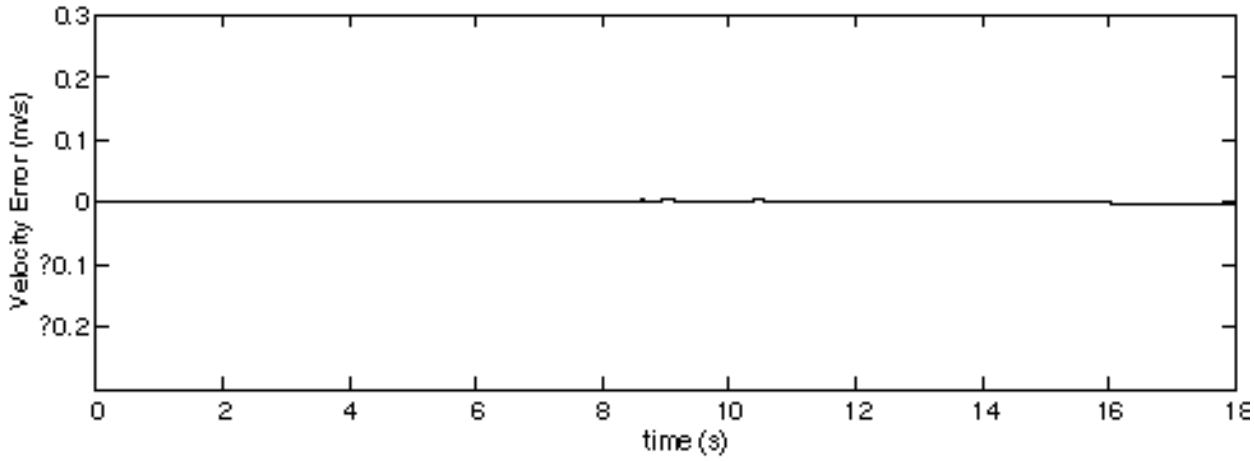

Figure 2.4 - Velocity Error Estimate, Profile Type 1 (v_f = 11.11 m/s), t_k Measurement Scenario 1

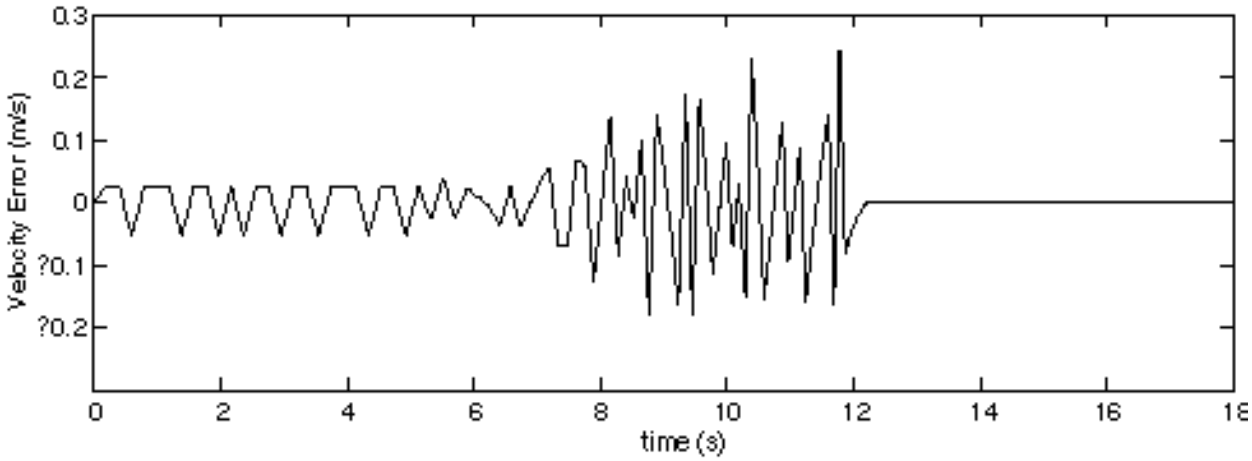

Figure 2.5 - Velocity Error Estimate, Profile Type 1 (v_f= 11.11 m/s), t_k Measurement Scenario 2

Both show nearly identical responses (zero error) once the final velocity is reached. Both simulations were run with the observer eigenvalues at the origin of the complex plane ("deadbeat" response). However, these results are misleading. If the velocity profile is changed slightly, so that v_f= 12 m/s, the results under scenario 2 are as shown in figure 2.6. Notice how, after the velocity change has been completed (at approximately 13 s), the velocity estimates are "switching" between two extreme values even though the vehicle is traveling at a constant velocity. In this case, the marker spacing ℓ is not an exact multiple of $v_f \times dt$; in fact, this corresponds to 27.78 cycles of 3 msec between markers. Because the readings occurred either at intervals of 27 or 28 cycles, the velocity estimates alternated between two different values. Therefore, the velocity error estimate as shown in the figure was unable to settle to zero, even though the vehicle was traveling at a constant velocity.

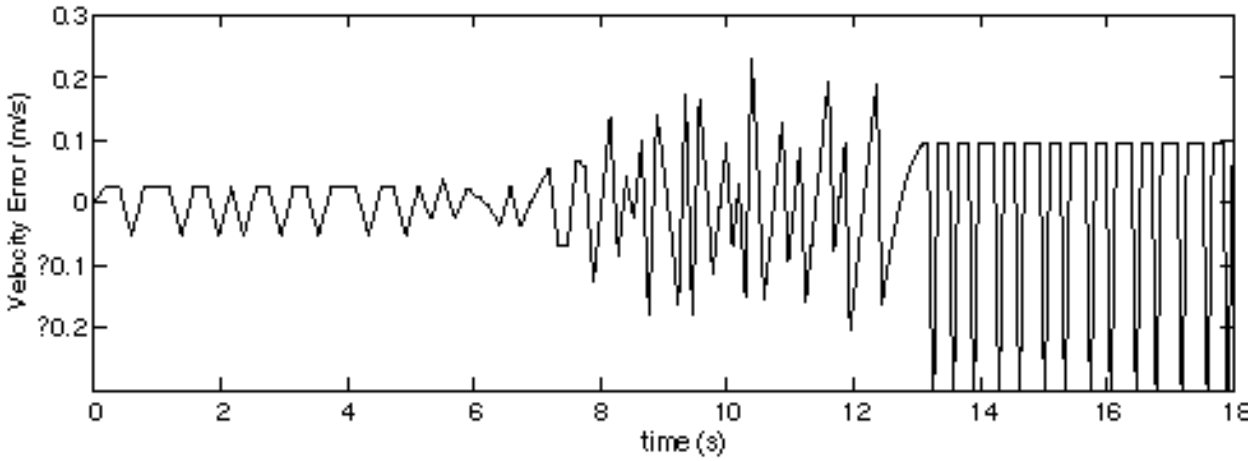

Figure 2.6 - Velocity Error Estimate, Profile Type 1 (v_f= 12 m/s),
t_k Measurement Scenario 2

A schematic of what is happening in general is shown in figure 2.7. The velocity estimate switches between two values (ℓ/4dt and ℓ/3dt) on either side of the true velocity (ℓ/3.5dt). The amount of time spent on each (incorrect) value is such that the integral of the error (in the long run) is zero, but the fact that the estimates are "oscillating" could make it very difficult to implement a controller based on these estimates. The concept of a "maximum spacing error" compensator was developed to reduce the effects of these incorrect estimates.

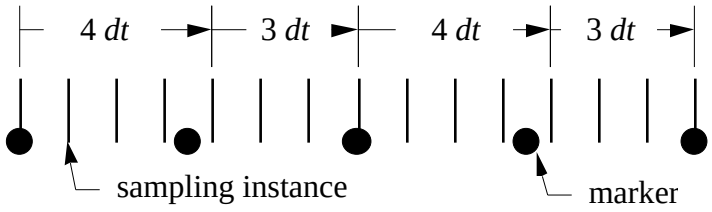

Figure 2.7 - Schematic of Oscillatory Velocity Estimates,
t_k Measurement Scenario 2

2.4 Maximum Spacing Error Compensation

While it is expected that the velocity estimate can be made smoother if we redesign an observer to incorporate tachometer feedback, it is shown that the information from the markers can be utilized more effectively to minimize the asynchronous effect discussed above. The algorithm which was implemented to compensate for this oscillatory behavior takes advantage of the fact that, if a vehicle is traveling at a constant velocity, the time between markers will vary by

no more than the sampling period, or one "tick" of the sampling clock. The positional uncertainty, or spacing error, created by these changing times can be no more than $v_f \times dt$, which obviously increases with higher velocities (see figure 2.8). In this algorithm, if the measured T_m varies by less than one "tick" from one marker to the next, the observer assumes that the vehicle is actually traveling at a constant velocity, and the new velocity estimate is calculated as the average of the current and previous estimates, rather than by the standard estimator given in Eq. (2.23).

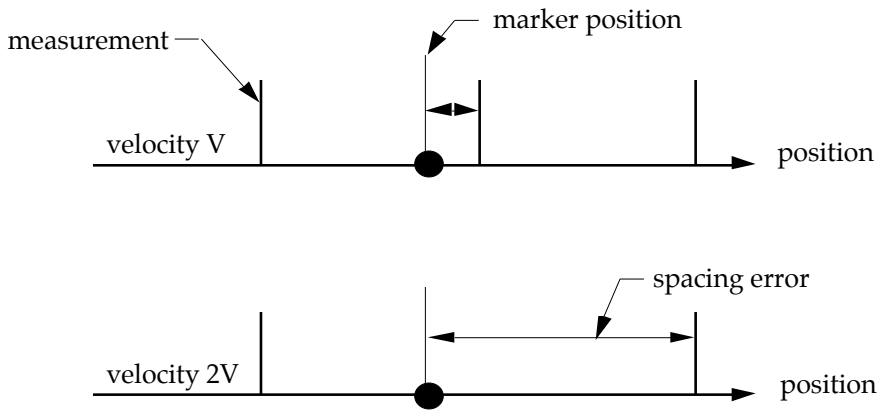

Figure 2.8 - Maximum Spacing Error

Figure 2.9 shows the response of the hybrid observer with maximum spacing error compensation to the exact same profile as was used in the generation of figure 2.6. At low velocities and high accelerations, the two observers yield identical estimates, but once the change in T_m became less than one "tick" per marker, the maximum spacing error compensation changed the estimates. This method is slower to respond during gradual acceleration and deceleration, because the assumption (by the compensator) of constant velocity is invalid, but it considerably reduces the variance of the velocity error.

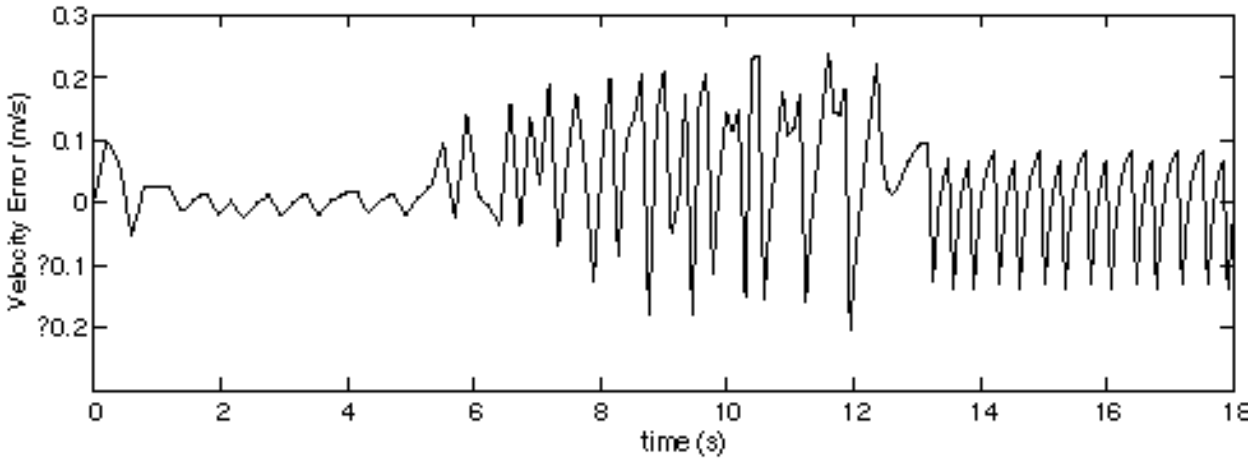

Figure 2.9 - Effect of Maximum Spacing Error Compensation

The "averaging" effect that the maximum spacing error compensator has on the state estimates can be seen more clearly by examining the true error more closely. Figure 2.10 shows a detail of one portion of a simulation, and clearly indicates the averaging effect that the compensator has. In the constant-velocity portion of figure 2.10 (after 15 seconds), the plot shows how the oscillatory effect is minimized. (The "spike" at 15 seconds is due to jerk as the vehicle suddenly stops accelerating.) The plot also hints at the reason why the observer is slower to respond during gradual acceleration: instead of converging asymptotically via the **[I - LC] $\mathbf{A_d}$** error dynamics, it merely averages between successive velocity estimates. This leads to a slightly higher average error than the observer without maximum spacing error compensation, but the variance is reduced significantly. This reduction in variance is desirable because it will help reduce subsequent control effort.

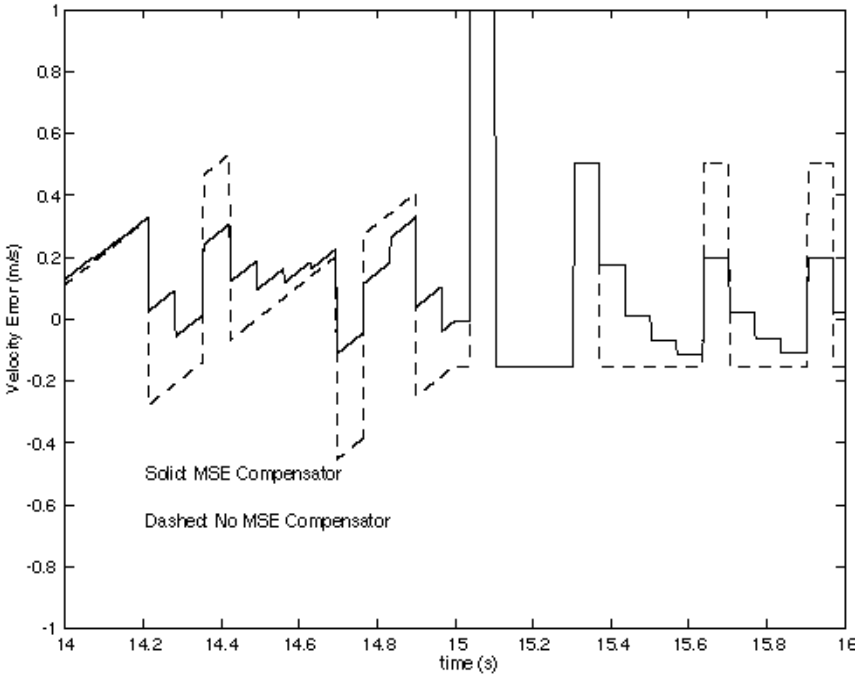

Figure 2.10 - Detail of Velocity Error

3.0 Longitudinal Controller Based on Discrete Markers

Once a feasible state estimator was developed, we began work on designing a controller which could use these state estimates for longitudinal control of a vehicle. In these simulations, the plant was again chosen as a pure inertial system, and the first t_k measurement scenario was used. Simulations using the second ("exact") t_k measurement scenario, both with and without maximum spacing error compensation, will be discussed in a later subsection. The controller structure was chosen as Proportional-Integral-Derivative (PID), because response characteristics could be predicted by examining pole placement.

3.1 Continuous-Time Controller as Reference Case

The first step in the development of a point-based longitudinal controller was to obtain a reference or "control" case, to determine how a continuous system responded to the commands that the discrete system would encounter. The basic structure of this controller is shown in figure 3.1.

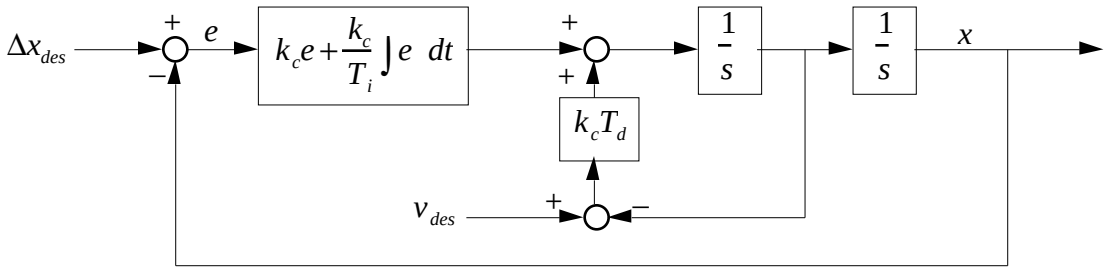

Figure 3.1 - Controller Structure

The primary longitudinal commands that a vehicle will have to accept are those of velocity change and marker advance/fallback. The first and most simplistic method of realizing a marker advance is to introduce a step change in desired position, and use the controller for disturbance rejection. For example, at time t_0, the controller is informed that the vehicle is a distance ($num \times \ell$) behind its desired position, where num is the number of markers and ℓ is the marker spacing. Because zero overshoot is desired, controller parameters k_c, T_i, and T_d are chosen so that the poles are strictly negative and real, and provide for a reasonable response time.

After these values were chosen, the controller was further tuned in simulation. The reason for this was the fact that limits on jerk and acceleration were imposed, to approximate more accurately the vehicle behavior and ride comfort limitations. In fact, even though the poles could analytically be placed with two at the breakpoint, giving the fastest transitional response, the jerk and acceleration limits slowed the response.

Some typical simulation results for this reference case are shown in figure 3.2. For this case, a marker spacing of ℓ = 1 m was assumed, and the command to move forward *num* = 10 markers was given at t_0 = 5 s. The vehicle was traveling at a constant velocity of v_{des} = 15 m/s before the advance command was given. It should be noted that, in this test case, a constant desired velocity v_{des} was assumed, and the marker advance command was viewed as a step disturbance of magnitude (*num* × ℓ). Therefore, Δx_{des} = (v_{des} × time) was the position command sent to the controller before the marker advance time, and Δx_{des} = (v_{des} × time) + (*num* × ℓ) was the command sent after the marker advance time. It should also be noted that

$$\frac{de}{dt} = \frac{d}{dt}\left(\Delta x_{des} - x\right) = v_{des} - v, \qquad 3.1$$

which implies that accurate instantaneous velocity measurements must be available. This structure was chosen over one with a direct derivative of the position error signal.

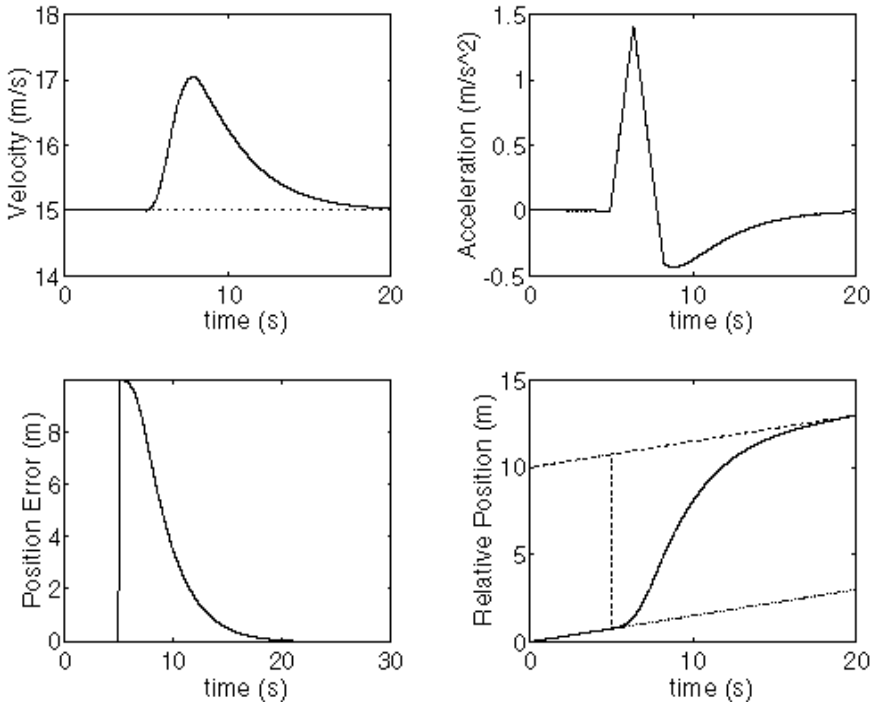

Figure 3.2 - Continuous Controller Simulation

3.2 Trajectory Definition

The next step in the controller design was to simulate the system when the instantaneous velocity was not available. In this case, the error would be interpreted as a "timing" error, or the difference between the time a vehicle was commanded to reach a given marker and the time when it actually reached that marker. Before this step could effectively be taken, a more precise definition of Δx_{des} and v_{des} was necessary. In other words, a desired profile had to be created. The "optimal" trajectory for this problem is a trapezoidal acceleration trajectory, because it gives a minimum-time transition from initial state to final state, with jerk and acceleration limits built in, rather than being applied as constraints after a controller has asked for a given jerk and acceleration. An example of a trapezoidal acceleration profile for advancing markers is shown in figure 3.3, along with its associated velocity and position profiles.

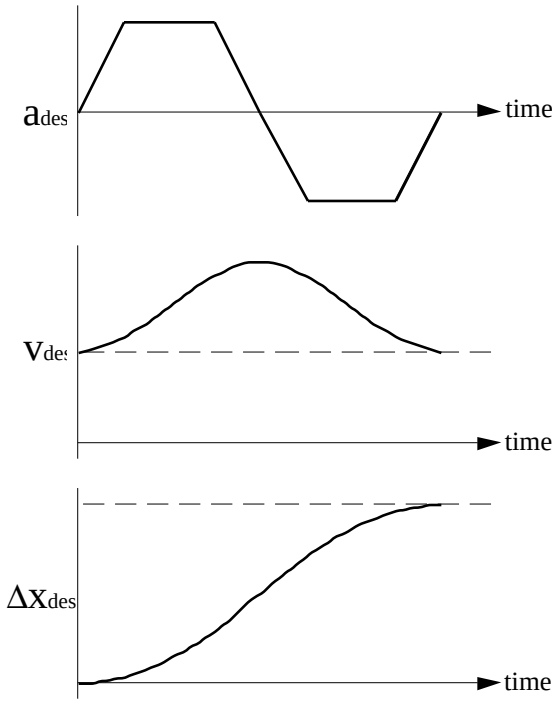

Figure 3.3 - Trapezoidal Acceleration Profile

This profile, which is fully defined for desired position, velocity, acceleration, and jerk, can be use to generate a synchronization pulse for single as well as multiple vehicle control. Referring to figure 1.1, if each vehicle shares the same pulse sequence during a series of maneuvers, each vehicle will need only a moderate-accuracy range sensor so that the controller can be aware of its position relative to adjacent vehicles. This higher-level platoon controller is an item for future research.

This trapezoidal profile was simulated using the same controller as in the previous subsection, and it gave marker advance trajectories as shown in figure 3.4. In this case, the acceleration was limited to 0.05 g rather than 0.1 g, yet the system showed approximately the same response time. The acceleration command is much cleaner than that of figure 3.2, indicating a more comfortable ride, and the vehicle never deviates from the commanded trajectory by more than 8 cm. In addition, the introduction of a feedforward controller will further reduce the tracking error.

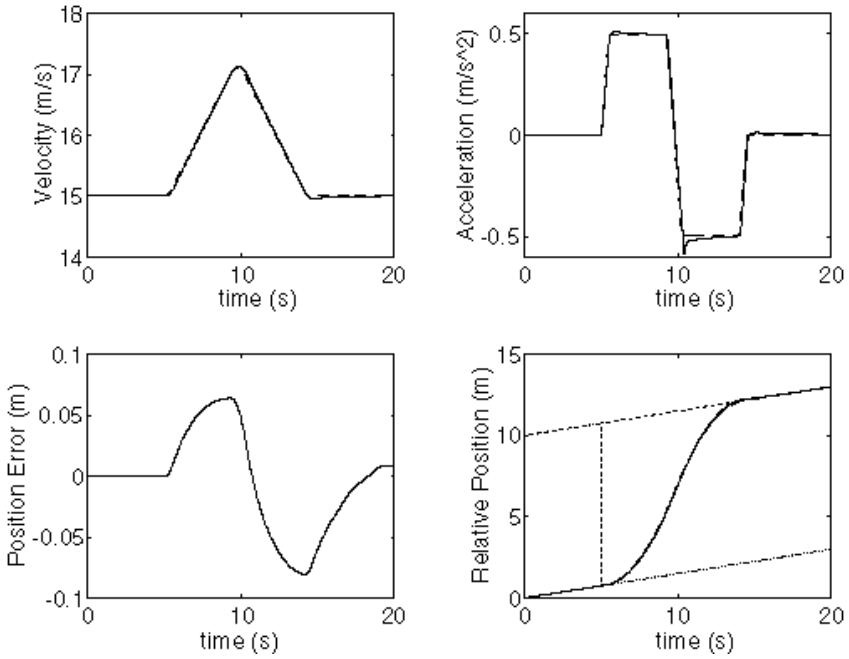

Figure 3.4 - Simulation Using Trapezoidal Acceleration

Figure 3.5 is a comparison between the continuous system response to both methods of commanding a marker advance. In this figure, the maximum allowable acceleration for the "Disturbance" profile was 0.15 g, whereas the "Trapezoidal" acceleration was limited to 0.08 g. This illustrates that the trajectory definition described above gives a significant improvement in response time, while still respecting both jerk and acceleration limits. Due to the fact that the error (position or timing) at any one instant is greatly reduced, the use of this profile also allows for the reduction of the controller gains.

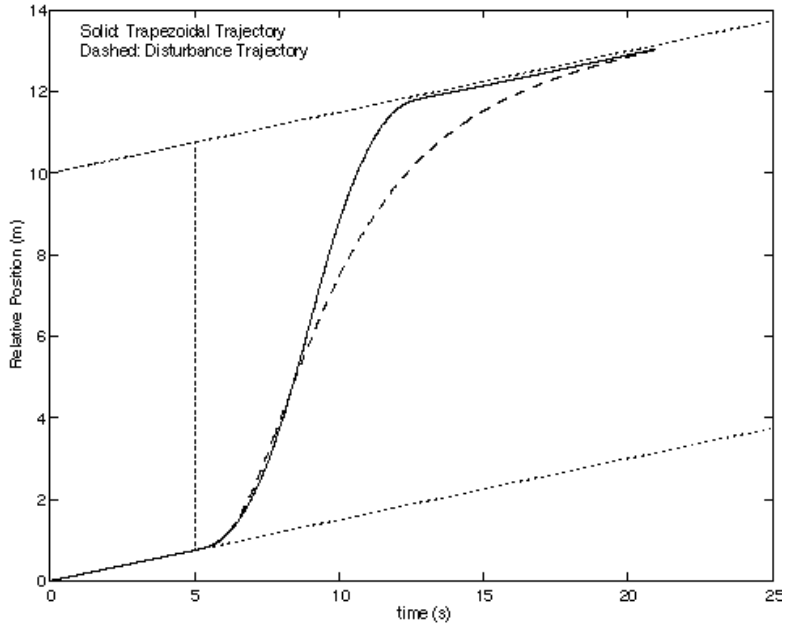

Figure 3.5 - Marker Advance Response, Trapezoidal Trajectory vs. Disturbance Rejection

3.3 Controller Based on Timing Error

Once the trapezoidal trajectory had been developed, the controller was moved into the discrete domain. For this case, the controller structure was as shown in figure 3.6, which is similar to figure 3.1. For this controller, however, the error signal was generated only when the vehicle passed a marker. If a good estimate of wheel slip can be obtained, the velocity estimate can be taken from a tachometer by use of Eq. (2.7).

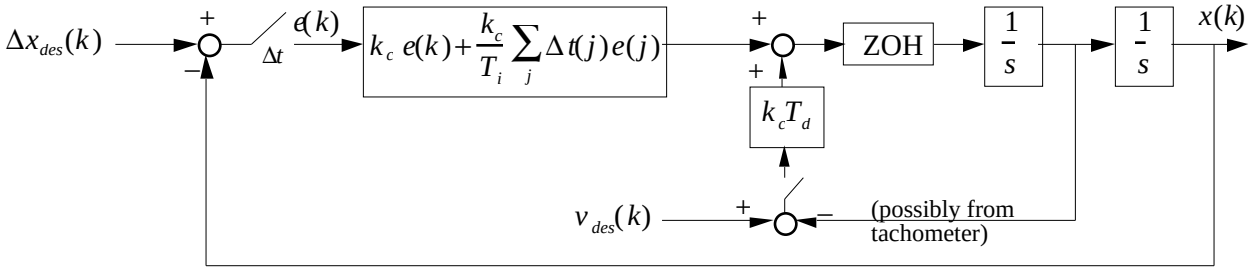

Figure 3.6 - Timing Error Controller Structure

In figure 3.6, the Δt term represents T_m if the control is updated only when the states are updated, but it could also represent dt or any other time interval over which the control is updated in multi-rate control. In this subsection, we assume that Δt is set equal to T_m. Notice

that under this assumption, the sampling period for the discrete-time control is not fixed. Discrete-time control with a fixed controller output update period, which is normally shorter than the measurement sampling period (T_m in the present problem), is called multi-rate control, and will be discussed in the next subsection.

The error signal for this controller can be written as

$$e(k) = T_e(k) \times v_{des}, \tag{3.2}$$

where $T_e(k) = t_{sp}(k) - t_k$ is the "timing error" for the k-th marker, and $t_{sp}(k)$ is the time of the k-th synchronization pulse, as mentioned in the previous subsection. The desired time between markers at any given point of a marker advance trajectory is

$$T_{m,des} = \frac{\ell}{v_{des}} = \frac{\ell}{(v_{des,c} + \Delta v_{des})}, \tag{3.3}$$

where $v_{des,c}$ is the desired cruising speed (e.g., platoon velocity) and Δv_{des} is the desired variation during the advancing maneuver. For a desired velocity profile like that shown in figure 3.3, this will generate a synchronization pulse sequence similar to that in figure 3.7.

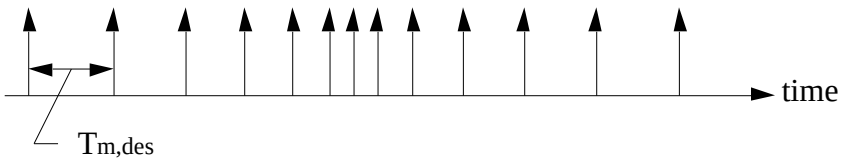

Figure 3.7 - Schematic of Timing Pulse Sequence

The results of a simulation of this controller are shown in figure 3.8. For this simulation, all parameters were identical to the scenario which was used in figure 3.2. As noted before, the derivative term in the PID controller includes velocity information. In this case, instead of using direct tachometer measurements, $v(k) = x_2(k)$ was estimated by $\hat{x}_2(k)$ in the first t_k estimation scheme. The controller parameters and commanded profile are identical to those used for the simulation which generated figure 3.4.

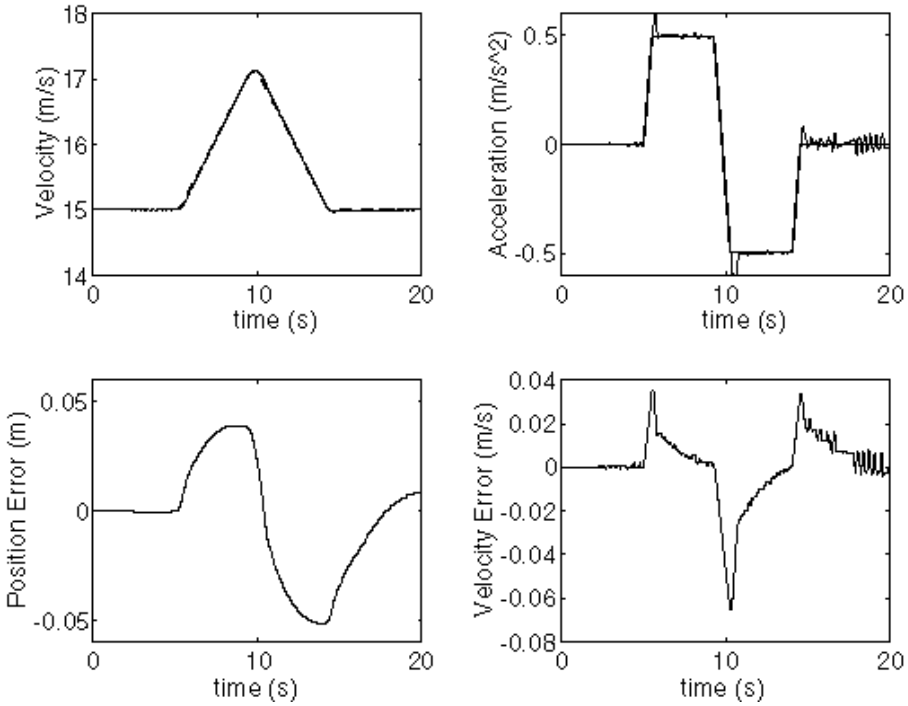

Figure 3.8 - Timing Error Controller Simulation

3.4 Multi-Rate Discrete Time Control Using the Hybrid Observer

The discrete time PID controller does not necessarily have to be implemented as in the last section. Instead, the controller output can be updated with a shorter update period than the measurement period. A hybrid observer plays a critical role in the implementation of a high frequency update rate for the controller output, due to the necessity for accurate state estimates between markers. Because of this accuracy requirement, the simulation was first run under the first t_k measurement scenario, i.e., exact measurement. A simulation scenario identical to that used for the generation of figures 3.4 and 3.8 was performed with the controller using this observer (shown in figure 2.1), and the results were essentially the same as those of figure 3.8, so are not plotted.

3.5 Effect of Acceleration and Jerk Limits

In order to make the vehicle model slightly more realistic than the pure inertial model, it is possible to introduce a limiter logic for both the vehicle acceleration and jerk (rate of change of

acceleration) into the feedback loop. While the limits placed on the desired trajectory design in section 3.2 are primarily for rider comfort, these new limits represent vehicle limitations only. In the previous controller simulations, the first, or exact, t_k measurement scenario was utilized, and the jerk and acceleration limits had no debilitating effects. However, when the measurement of t_k is changed to the second, or approximate, scenario, the controller is not able to stabilize the vehicle for even a simple maneuver, as shown in figure 3.9. Even the reduction in error variance due to the use of the maximum spacing error compensation scheme is not enough to counteract the adverse effects of the artificially imposed jerk limit.

The combination of short marker spacing and relatively high velocity gives a very high-frequency signal to the controller, and these inexact estimates behave as a "bounded" measurement noise. Even though a bounded noise cannot make a stable system unstable, any assumed stability due to the PID pole placement is rendered invalid by the jerk and acceleration limits, and in fact the vehicle can become unstable. Because the velocity estimates and commanded accelerations are switching so rapidly, the desired acceleration cannot be reached due to the jerk limit. If the "exact" t_k measurement scenario is used, this noise-like uncertainty is not present. It appears, therefore, that to maintain rider comfort and respect vehicle limitations during routine maneuvers, accurate knowledge of marker location, or at least more accurate than 3 msec, is vital to system stability.

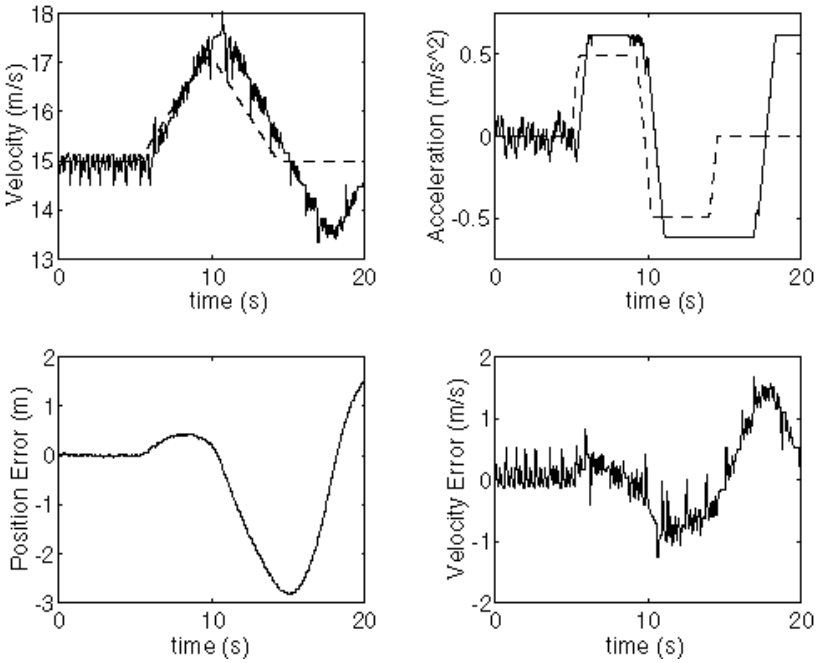

Figure 3.9 - Multi-Rate Control Using
t_k Measurement Scenario 2

4.0 Concluding Remarks

The studies of the past year have shown that through the use of a hybrid observer, position and velocity estimates of a simple vehicle model can be obtained with reasonable accuracy. Setting the eigenvalues of the error matrix to the origin of the complex plane introduces finite settling time, or deadbeat, response, which decouples the velocity and position estimates. This decoupling allows for easier fault detection within the observer. Accurate measurement of the precise time when a vehicle passes over a given marker is not strictly necessary for the observer, and methods have been developed to minimize the error created by this inexact measurement.

Jerk and acceleration limits, imposed both by vehicle capabilities and rider comfort, restrict the range of allowable commands that the controller can accept. If tracking errors become large, these limitations on the speed of the controller response can change the system behavior, and decrease robustness. This reduction in robustness becomes more prominent when the vehicle is traveling at high velocities with short marker spacings. In these cases, even if the exact marker timing is found errors can arise between the time the measurement is taken and the next tick, when it is utilized, because though the vehicle acceleration can be measured, uncertainties propagate during the prediction portion of the observer. In addition, because of the sparseness of input signals, long marker spacings make low-velocity tracking difficult.

The restrictions due to jerk and acceleration limits can be partially negated by using them as part of a trajectory design. It is still possible for the controller to ask for accelerations beyond those specified by the trajectory, but if the trajectory is designed so that the commanded accelerations are below both vehicle and rider comfort limits, the proper choice of controller parameters will keep the actual accelerations to a reasonable level. Additionally, if accurate marker spacing is determined, perhaps with the use of a hardware peak detector, devices such as maximum spacing error compensation become unnecessary.

Control of the vehicle, though PID in structure, can be done effectively both as discrete-time control (control is updated at the same rate as the state estimates) and multi-rate control (control is updated at a different rate from the state update rate). In the limit, a multi-rate controller will recalculate the desired control every time the predictor is updated, so the accuracy of the hybrid observer is vital to controller performance. For the controller which was developed, obtaining very accurate marker timing is a necessity for good performance.

References

[1] Chang, K.-H. and C. N. Georghiades. 1992. "A Position Estimation Algorithm for Vehicle Following", *Proceedings of the 1992 American Control Conference*, Chicago, pp. 1758-1762.

[2] Chien, C. C., and P. Ioannou. 1992. "Automatic Vehicle-Following", *Proceedings of the 1992 American Control Conference*, Chicago, pp. 1748-1752.

[3] Hedrick, J. K. et al. 1991. "Longitudinal Vehicle Controller Design for IVHS Systems" *Proceedings of the 1991 American Control Conference*, Boston, pp. 3107-3112.

[4] Hessburg, T. et al. 1991. "An Experimental Study on Lateral Control of a Vehicle" *Proceedings of the 1991 American Control Conference*, Boston, pp. 3084-3089.

[5] McMahon, D. H. et al. 1990. "Vehicle Modelling and Control for Automated Highway Systems" *Proceedings of the 1990 American Control Conference*, San Diego, pp. 297-303.

[6] McMahon, D. H. et al. 1992. "Longitudinal Vehicle Controllers for IVHS: Theory and Experiment" *Proceedings of the 1992 American Control Conference*, Chicago, pp. 1753-1757.

[7] Ogata, K. 1987. *Discrete-Time Control Systems*, Chapter 6, Prentice-Hall.

[8] Peng, H. and M. Tomizuka. 1991. "Preview Control for Vehicle Lateral Guidance in Highway Automation" *Proceedings of the 1991 American Control Conference*, Boston, pp. 3090-3095.

[9] Peng, H. et al. 1992a. "A Theoretical and Experimental Study on Vehicle Lateral Control" *Proceedings of the 1992 American Control Conference*, Chicago, pp. 1738-1742.

[10] Peng, H. et al. 1992b. "Experimental Automatic Lateral Control System for an Automobile" University of California at Berkeley: Institute of Transportation Studies, California PATH Program. UCB-ITS-PRR-92-17.

[11] Sheikholeslam, S. and C. A. Desoer. 1992. "Combined Longitudinal and Lateral Control of a Platoon of Vehicles" *Proceedings of the 1992 American Control Conference*, Chicago, pp. 1763-1767.

[12] Tomizuka, M. and J. K. Hedrick. 1993. "Automated Vehicle Control for IVHS Systems" IFAC Conference, Sydney, Australia.

[13] Whitney, D. E. and M. Tomizuka. 1972. "Normal and Emergency Control of a String of Vehicles by Fixed Reference Sampled-Data Control" *IEEE Transactions on Vehicular Technology*, Vol. VT-21, No. 4, pp. 128-138.